A study on active structural acoustic control using force radiation modes

Rongfu Mao[1], Haichao Zhu[2], Shanping Gao[3], Xing Zhang[4]
[1, 3, 4]School of Mechanical and Electrical Engineering, Quanzhou University of Information Engineering, Quanzhou 362000, China
[2]Institute of Noise and Vibration, Naval University of Engineering, Wuhan 430033, China
[3]Corresponding author
E-mail: [1]*maorfu@163.com*, [2]*haiczhu@163.com*, [3]*345619197@qq.com*, [4]*448495290@qq.com*

Received 23 May 2024; accepted 15 September 2024; published online 6 October 2024
DOI https://doi.org/10.21595/jve.2024.24214

Abstract. Active Structural Acoustic Control (ASAC) is an effective method for sound radiation control. To solve the coupling effect or inconvenience problems existed in the application of conventional methods, by utilizing the characteristic of intuitive representation of radiated sound power through force radiation modes, the control forces are designed to make the total excitation force vector orthogonal to each dominant force radiation mode. Therefore, an ASAC method by utilizing force radiation modes is proposed, and detailed theoretical research and numerical calculation analysis are carried out. The research results indicate that the control force requirement can be intuitively obtained through the force radiation modes, and decoupled control of radiated sound power corresponding to each force radiation mode is achieved by the proposed method. Thus, the control strategy and system construction can be greatly simplified, and structural acoustic radiation can be effectively controlled.

Keywords: force radiation modes, active structural acoustic control, decoupling, radiated sound power.

1. Introduction

At present, high-end equipment is increasingly developing in the direction of high speed, heavy load, lightweight and extreme operating environment, which brings more serious structural vibration and noise problems. In especial, the effective control of low-frequency vibration and noise problems is an urgent problem to be solved. Active structural acoustic control (ASAC) is an effective acoustic control method with little influence on physical characteristics of the controlled system, which can make up for the shortcomings of traditional control methods and has advantages of satisfactory control effect in low and medium frequency band.

Fuller [1] took the lead in the ASAC theoretical study, demonstrating that it was possible to suppress the sound radiation of structure by applying secondary force sources to the surface of vibrating structure and achieve noise control in the sound field. Wu adopted a structural noise reduction approach by simultaneously modifying the structural modal velocity distribution and the system capability of disturbance rejection through active left-right eigenvector assignment control actions [2]. Bai also proposed an ASAC scheme, in which the left eigenvectors of a closed loop system were controlled to be orthogonal with the excitation force vector for the active structural acoustic control by use of the dependent modal space control method [3]. By taking advantage of the fact that decoupling between structural vibration and acoustic radiation can be realized, many scholars have made extensive researches on ASAC based on acoustic radiation mode (ARM) and many constructive research results were achieved [4-7]. In recent years, with the rapid development of acoustic metamaterial theory, various types of actively tuned acoustic metamaterial have also been utilized to conduct ASAC research [8-10], which further enriching the theoretical research and engineering application of ASAC.

From the control target view, the existed ASAC researches can be divided into two categories roughly: acoustic power components control by structural mode (SM) and ARM. Because of the

coupling relationship between SM and radiated sound power, noise reduction is not assured in SM based ASAC methods. For the ARM based ASAC methods, although the decoupling control of the radiated acoustic power can be realized, the distribution information of control forces cannot be intuitively determined, and there are still some inconvenient problems in practical application.

Yamaguchi [11, 12] introduced structural admittance matrix to extend the concept of ARM to force radiation mode (FRM), and stated out that FRM method was the most effective means to analyze the relationship between excitation force distribution and radiated sound power. Ji used the FRM to study the influence law of excitation force on structural sound radiation and the design of low noise structure [13, 14]. Since the radiated sound power is expressed by the excitation force as the variable, FRM represents the relationship between the excitation force and the radiated sound power more intuitively, and it is also convenient to obtain the control force distribution requirements in ASAC. According to above facts, FRM is introduced into ASAC in this paper, relevant theoretical study and numerical simulation are conducted in detail, and an FRM based ASAC method is proposed by configuring the control force distribution to make the total excitation force vector orthogonal to each dominant FRM.

2. Theories

2.1. Basic concepts

Consider an arbitrary vibrator structure immerged in homogeneous fluid with sound velocity c_0 and density ρ_0, radiating in free space at frequency ω. If the vibrating surface is discritized into N elements, the surface pressure vector $\mathbf{p}$ can be expressed by normal velocity vector $\mathbf{v}_n$ ($e^{-i\omega t}$ is assumed for simple form):

$$\mathbf{p} = \mathbf{Z}\mathbf{S}\mathbf{v}_n = (\mathbf{R}' + j\mathbf{X}')\mathbf{S}\mathbf{v}_n, \tag{1}$$

where, $j = \sqrt{-1}$, $\mathbf{p}$ and $\mathbf{v}_n$ are $(N \times 1)$ vectors of surface pressure and normal velocity on the discritized vibrating boundary surface respectively, $\mathbf{S}$ is an $(N \times N)$ diagonal matrix with area of the i-th element s_i $(i = 1,2, \ldots, N)$ in diagonal position, $\mathbf{Z}$ is an $(N \times N)$ impedance matrix of the vibrating structure surface with real part matrix $\mathbf{R}'$ and imaginary part matrix $\mathbf{X}'$.

The radiated sound power W can be obtained by surface pressure $\mathbf{p}$ and normal velocity $\mathbf{v}_n$:

$$W = \frac{1}{4}[\mathbf{p}^{\mathrm{T}}\mathbf{S}\mathbf{v}_n^* + \mathbf{p}^{\mathrm{H}}\mathbf{S}\mathbf{v}_n], \tag{2}$$

where, superscript "*", "T" and "H" denote conjugate transpose and conjugate transpose operator respectively.

Substituting Eq. (1) into Eq. (2), then the radiated sound power W can be obtained as:

$$W = \frac{1}{2}\mathbf{v}_n^{\mathrm{H}}\mathbf{S}\mathbf{R}'\mathbf{S}\mathbf{v}_n = \mathbf{v}_n^{\mathrm{H}}\mathbf{R}\mathbf{v}_n, \tag{3}$$

where $\mathbf{R} = \mathbf{S}\mathbf{R}'\mathbf{S}/\mathbf{2}$, which is an $(N \times N)$ real symmetric matrix.

The relationship between normal velocity $\mathbf{v}_n$ and excitation force $\mathbf{F}$ can be expressed as:

$$\mathbf{v}_n = \mathbf{G}\mathbf{Q}\mathbf{F}, \tag{4}$$

where $\mathbf{G}$ is an $(N \times N)$ coordinate transformation matrix, and $\mathbf{Q}$ is structural admittance matrix.

Substituting Eq. (4) into Eq. (3), the radiated sound power W can be rewritten as:

$$W = \mathbf{F}^{\mathrm{H}}\mathbf{Q}^{\mathrm{H}}\mathbf{G}^{\mathrm{T}}\mathbf{R}\mathbf{G}\mathbf{Q}\mathbf{F} = \mathbf{F}^{\mathrm{H}}\mathbf{T}\mathbf{F}, \tag{5}$$

where $\mathbf{T} = \mathbf{Q}^{\mathrm{H}}\mathbf{G}^{\mathrm{T}}\mathbf{R}\mathbf{G}\mathbf{Q}$, which is an $(N \times N)$ Hermitian matrix. From the physical definition of the acoustic power W in Eq. (5), it can be deduced that $W > 0$ will be always true except the excitation force vector equals 0. Therefore, $\mathbf{T}$ is positive definite and Hermitian, and it can be expressed by the eigenvalue decomposition as:

$$\mathbf{T} = \mathbf{D}\mathbf{A}\mathbf{D}^{\mathrm{H}}, \tag{6}$$

where $\mathbf{A}$ is a diagonal matrix with eigenvalues λ_i $(i = 1,2, \ldots, N)$ decreasing monotonically along the diagonal, $\mathbf{D}$ represents an $(N \times N)$ matrix whose columns are eigenvectors $\mathbf{d}_i$ $(i = 1,2, \ldots, N)$. Since $\mathbf{T}$ is positive definite and Hermitian, all of its eigenvalues λ_i are positive real and its eigenvectors $\mathbf{d}_i$ are orthogonal to each other. Each eigenvector $\mathbf{d}_i$ represents a particular excitation force pattern on the vibrating surface, so it's termed as Force Radiation Mode specifically.

From Eq. (5), matrix $\mathbf{T}$ depends on matrix $\mathbf{Q}$ and $\mathbf{R}$. By the definition, $\mathbf{Q}$ is related to the stiffness matrix and mass matrix of the structure, while $\mathbf{R}$ is related to the geometry of the vibrating surface and excitation frequency. Therefore, FRMs are not only dependent on the geometry and excitation frequency but also the material properties and boundary conditions of the flexible structure.

2.2. Decoupling control of acoustic radiation

Substituting Eq. (6) into Eq. (5), the radiated sound power W becomes:

$$W = \mathbf{F}^{\mathrm{H}}\mathbf{D}\mathbf{A}\mathbf{D}^{\mathrm{H}}\mathbf{F} = \mathbf{y}\mathbf{A}\mathbf{y}^{\mathrm{H}} = \sum_{i=1}^{N} \lambda_i |y_i|^2, \tag{7}$$

where $\mathbf{y} = \mathbf{F}^{\mathrm{H}}\mathbf{D}$, which is the amplitude coefficient matrix of FRM. As can be seen from Eq. (7), the total radiated sound power is the sum of corresponding components of each order of FRM, and there is no spillover effect between each FRM, which means the radiated sound power can be decoupled by the FRMs. In practical applications, since the first several eigenvalues are far larger than others, the radiated sound power would be mainly contributed by corresponding dominant FRMs.

Supposing the total excitation force distribution on the flexible structure is composed by m primary forces $\mathbf{F}_p$ and n secondary control forces $\mathbf{F}_s$:

$$\mathbf{F} = \mathbf{F}_p + \mathbf{F}_s. \tag{8}$$

Combining Eq. (7) and Eq. (8), the sound power W can be written as a Hermitian quadratic form with the secondary control force $\mathbf{F}_s$ as the independent variable:

$$W = \mathbf{F}_s^{\mathrm{H}}\mathbf{a}_A\mathbf{F}_s + \mathbf{F}_s^{\mathrm{H}}\mathbf{b}_A + \mathbf{b}_A^{\mathrm{H}}\mathbf{F}_s + \mathbf{c}_A, \tag{9}$$

where:

$$\mathbf{a}_A = \mathbf{D}\mathbf{A}\mathbf{D}^{\mathrm{H}}, \tag{10}$$
$$\mathbf{b}_A = \mathbf{D}\mathbf{A}\mathbf{D}^{\mathrm{H}}\mathbf{F}_p, \tag{11}$$
$$\mathbf{c}_A = \mathbf{F}_s^{\mathrm{H}}\mathbf{D}\mathbf{A}\mathbf{D}^{\mathrm{H}}\mathbf{F}_p. \tag{12}$$

According to the quadratic optimal theory, the optimal secondary control force $\mathbf{F}_{so}$ can be obtained by minimizing the radiated sound power W:

$$\mathbf{F}_{so} = -\mathbf{a}_A^{-1}\mathbf{b}_A. \tag{13}$$

The minimum value of the radiated sound power W_{min} is:

$$W_{min} = c_A - \mathbf{b}_A^{\mathrm{H}}\mathbf{a}_A^{-1}\mathbf{b}_A. \tag{14}$$

It can be seen from the observation of Eq. (7) that the perfect ASAC control can be obtained if the corresponding FRM amplitude can be set to 0. To satisfy this condition, in addition to making the control force $\mathbf{F}_s = -\mathbf{F}_p$ (both applied at the same position, with equal magnitude and opposite direction), we can also make the total excitation force vector **F** orthogonal to each dominant FRM by assigning a certain secondary control force distribution.

For acoustic radiation problems, the radiated acoustic field is generated by the excitation forces. Fig. 1 compares the principles of several common ASAC methods. As can be seen from the figure, in the SM control methods, the radiated sound power W is obtained by structural mode amplitude (thus vibration response) in a quadratic form indirectly. Coupling occurs not only between control force and vibration response, but also between vibration and acoustic radiation in the SM control methods. Therefore, the control spillover effect is very significant, and the control system design will be very complicated. For the ARM control methods, the radiated sound power W is obtained by normal velocity in a quadratic form indirectly. Decoupling of structural vibration and acoustic radiation can be realized, and its control system design is simpler than the SM control method, but there is still coupling between the control force and the structural vibration response, and the control spillover effect also appears, so it is still difficult to realize the decoupling control of acoustic radiation. Different from the two mentioned methods, the radiated sound power W is obtained by excitation force **F** in a quadratic form directly, decoupling relationship between the control force and the sound radiation is established by using the FRM control method without the coupling effect, which can greatly simplify the control system and improve the control effect and robustness. This is the exact advantage of using the FRM control method for sound radiation analysis and control.

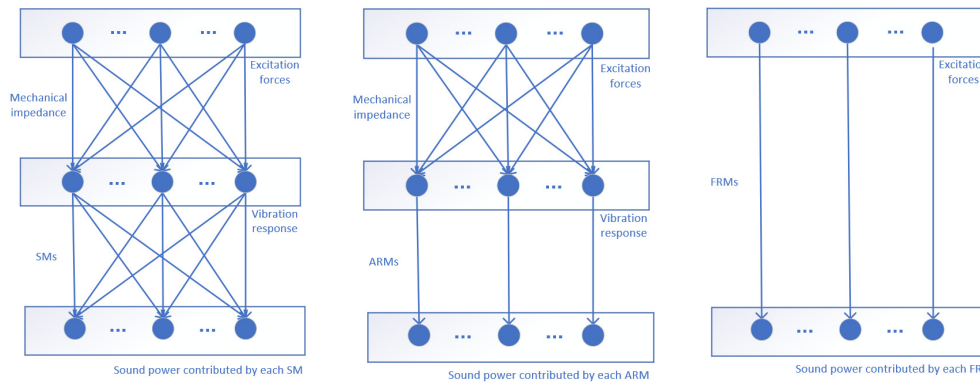

a) SM control methods b) ARM control methods c) FRM control methods

Fig. 1. The principles comparison of different ASAC methods

3. Numerical simulations

3.1. Simulation settings

The numerical simulation and analysis of ASAC using FRM control methods are carried out by taking a rectangular simply supported plate excited by vertical harmonic point force as an example. The plate size is 1.0 m (L_x)×0.8 m (L_y), and the thickness h is 0.005 m. The primary excitation force $\mathbf{F}(t) = Fe^{j\omega t}$ is a single simple harmonic force with amplitude $F = 1$ N, applied

ISSN PRINT 1392-8716, ISSN ONLINE 2538-8460

near a corner $(L_x/4, L_y/4)$ of the flexible plate. The density of the air medium ρ_0 is 1.21 kg/m^3, and the sound velocity c_0 is 343 m/s. The parameters of the plate material are as follows: Young's modulus E is 2×10^{11} Pa, Poisson's ratio ν is 0.28, density ρ is 7800 kg/m^3. The first 6 structural modal frequencies are shown in Table 1.

Table 1. The first 6 structural modal frequencies

Order	(1, 1)	(1, 2)	(2, 1)	(2, 2)	(1, 3)	(3, 1)
Modal frequency / Hz	30.6	66.5	86.7	122.6	126.3	180.1

As know from the acoustic radiation law of the plate, the radiation efficiency of odd-odd modes is much higher than that of odd-even and even-odd modes at low frequencies. Therefore, the FRM and its ASAC control are calculated and analyzed at typical odd-odd, odd-even(odd-even), even-even modal frequencies and non-modal frequencies.

3.2. FRM calculations

According to the theoretical method described in this paper, the FRMs of (1, 1), (2, 1), (2, 2) order modal frequencies and non-modal frequency at 100 Hz are calculated respectively. The amplitude distributions of the first four FRMs are illustrated in Fig. 2(a-d) respectively. It can be seen from the figures that each order of FRM will change significantly at different frequencies. At the modal frequencies, the 1st FRM exhibits high consistency with corresponding SM, and the higher-order FRMs show similar modal shapes with the SMs at adjacent modal frequencies. However, at the non-modal frequencies, the 1st FRM is not necessarily similar to the SMs at the adjacent modal frequencies, while the higher-order FRMs still show similar modal shapes with the SMs at adjacent modal frequencies.

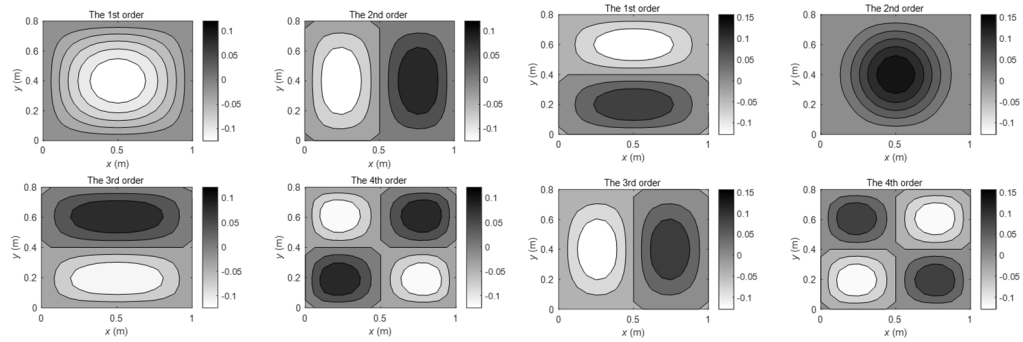

a) At (1, 1) modal frequency

b) At (2, 1) modal frequency

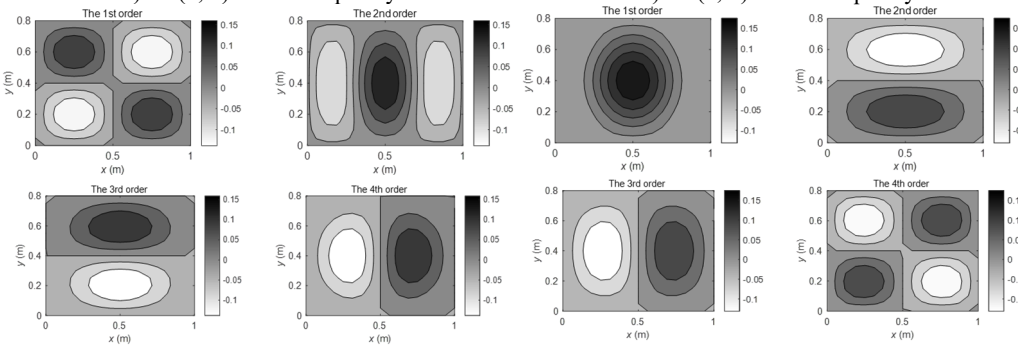

c) At (2, 2) modal frequency

d) At non-modal frequency 100 Hz

Fig. 2. The FRM amplitude distributions at typical frequencies

Considering frequency range 20 Hz-200 Hz, Fig. 3 gives the eigenvalues changing with frequency corresponding to the first 6 FRMs of the plate. As can be seen from the figure, after mathematical eigenvalue decomposition, the eigenvalues corresponding to the 1st FRM are always the largest, and show peak values at corresponding modal frequencies. The eigenvalues corresponding to the higher order FRMs decrease with the increasing order. At odd-odd modal frequencies, the eigenvalues corresponding to the higher-order FRMs decrease the most with the increasing order, followed by odd-even (even-odd) modal frequencies, and at even-even and non-modal frequencies, and the eigenvalues decrease more slowly. The above results show that it is only necessary to consider the contribution of the 1st or a first few dominant FRMs in the ASAC control at odd-odd and odd-even (even-odd) modal frequencies, however, more FRMs may need to be considered at even-even and non-modal frequencies.

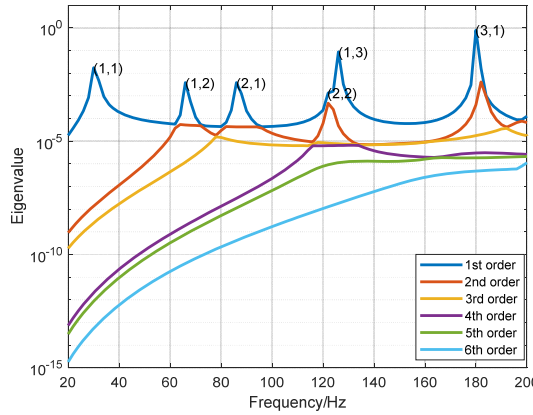

Fig. 3. The eigenvalues corresponding to the first 6 FRMs

3.3. ASAC results

Suppose the flexible plate is evenly divided into 5×5 grids. Since four edges of the plate are simply supported, the actual required control force distribution for ASAC is 3×3. Then ASAC of the plate under the primary excitation force is simulated by exploiting the FRM control method presented in this paper.

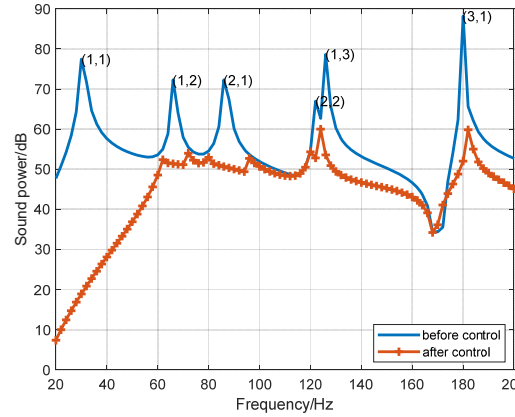

Fig. 4. The radiated sound power curve before and after control

If only the acoustic power contributed by 1st FRM is controlled, the radiated sound power curves before and after control are shown in Fig. 4, and the detailed acoustic power reduction

results at typical modal frequencies and non-modal frequency of 100 Hz are given in Table 2. As can be seen from the Fig. 4, control of the 1st FRM contributed sound power can already achieve satisfactory reduction results at all modal frequencies, but the control effect is still limited at non-modal frequencies, the acoustic power reduction at 100 Hz is only 1.2 dB as shown in Table 2. The explanation is that the number of dominant FRMs is greater than the number that has been controlled at the non-modal frequencies.

Table 2. Acoustic power reduction at typical frequencies ($W_{ref} = 10^{-12}$ W)

Modal order / Frequency	(1, 1)	(1, 2)	(2, 1)	(2, 2)	(1, 3)	(3, 1)	100 Hz
Reduction (dB)	58.5	20.9	21.6	14.2	25.0	36.1	1.2

In the following parts, the mechanism of ASAC using FRM control methods is further analyzed combined with the simulation results.

Firstly, take control case at (1, 1) modal frequency of 30Hz as an example. As can be seen from the detailed results in Table 2, satisfactory control effect can already be obtained when the 1st FRM is controlled, the radiated sound power of the plate can be reduced by 58.5 dB. The vibration velocity distributions on the plate before and after ASAC control are illustrated in Fig. 5. It can be observed that the vibration velocity of the plate also attenuates greatly after control, and the RMS value of the vibration velocity decreases from 3.1 mm/s before control to 0.1 mm/s after control. The comparison of amplitudes of FRMs and SMs before and after control are further shown in Fig. 6. It can be noted from Fig. 6(a) that the amplitude of the 1st FRM is reduced significantly, while the amplitudes of higher orders of FRMs remain almost unchanged. According to eigenvalue curves of each FRMs in Fig. 3, it can be seen that the eigenvalues of the 1st FRM are much higher than that of the higher order FRMs. Therefore, the total sound power can be effectively attenuated when the 1st FRM contributions is suppressed. On the other hand, as described in Fig. 6(b), the amplitude of (1, 1) SM (contributing the most to the vibration before control) is suppressed obviously, while the amplitudes of other SMs are nearly the same. Accordingly, the vibration on the plate can also be well controlled, which is consistent with the result in Fig. 5(b). Combing above analysis of results in Fig. 6(a) and Fig. 6(b), it can be deduced that the sound radiation and vibration of the plate can both be controlled effectively at the same time with the presented FRM controlled ASAC method, since that the 1st FRM is similar to the SM at the studied modal frequency.

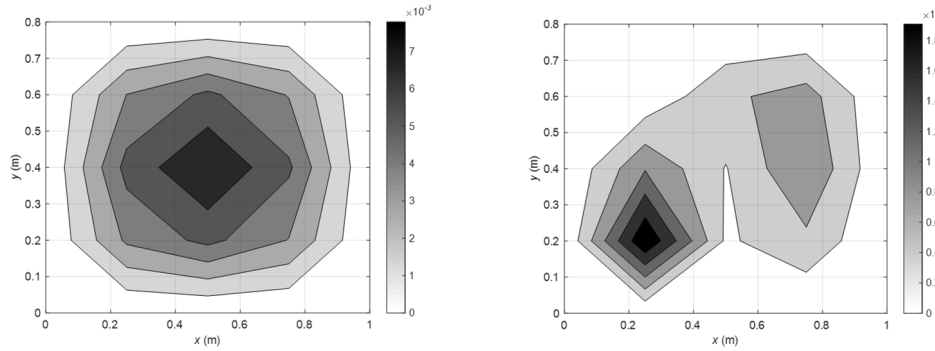

a) Before control b) After control

Fig. 5. The vibration velocity distributions on the plate (30 Hz)

Secondly, control case at the non-modal frequency of 100 Hz is investigated. When the 1st FRM is controlled, the radiated sound power of the plate decreases by only 1.2 dB, as shown in Table 2. The reason can be found in Fig. 3, it is shown that there are 3 FRMs with relatively large eigenvalues at this frequency, which are more than the number that has been controlled. Therefore, the final sound radiation control is not so good in this condition. If the control targets are extended

to the first 3 FRMs, the sound power reduction will be improved to 26.2 dB, and the vibration velocity distributions on the plate before and after the control are depicted in Fig. 7. As can been found that the vibration velocity of the plate is attenuated in a small extent after the control, and the RMS value of the vibration velocity decreases only from 0.3mm/s before control to 0.2 mm/s after control. Once again, the comparison of amplitudes of FRMs and SMs before and after control are further demonstrated in Fig. 8. As illustrated in Fig. 8(a), the amplitudes of the first 3 FRMs with relatively large eigenvalues are all significantly attenuated, while the amplitudes of the other FRMs almost stay unchanged. Consequently, the total sound power is assured to be effectively controlled. Meanwhile, as shown in Fig. 8(b), the amplitudes of (1, 2) and (2, 1) SMs (contributing largely to the vibration before control) are significantly attenuated, (1, 1) SM is also suppressed in a certain extent, while the amplitude of (2, 2) SM that also contributes a lot to vibration remains almost the same.

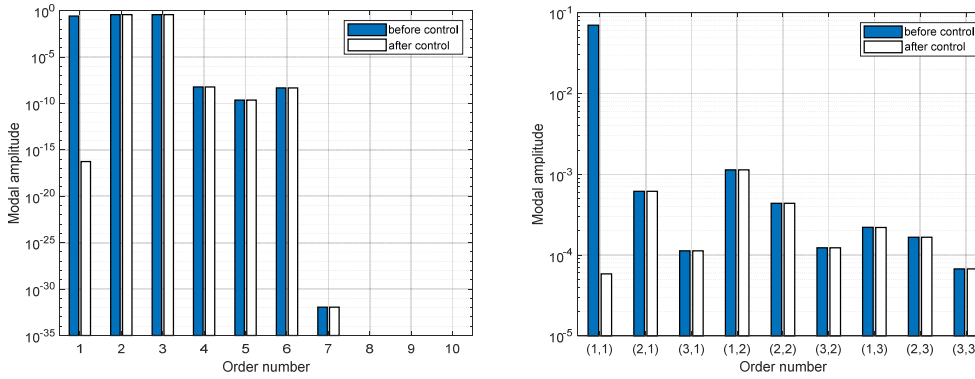

a) Amplitude of FRMs b) Amplitude of SMs

Fig. 6. Comparison of amplitudes of FRMs and SMs before and after the control (30 Hz)

According to the acoustic radiation law of plate in low frequency band, the odd-odd SMs possess the highest radiation efficiency, followed by odd-even (even-odd) SMs, and even-even SMs show the lowest one. Therefore, when the odd-odd and odd-even (even-odd) SMs with higher radiation efficiency are controlled, the acoustic radiation can be effectively controlled. However, as the even-even SMs that also contribute largely to vibration of the plate remain unattenuated, the vibration control effect is not as good as the (1, 1) modal frequency case. Combing above analysis of results in Fig. 8(a) and Fig. 8(b), it can be deduced that the sound radiation of the plate can be attenuated greatly by controlling the first several FRMs with relatively large eigenvalues, while the vibration control effect is not assured as good as that at the modal frequency, since the 1st FRM is not necessarily similar to the SMs at the adjacent modal frequencies.

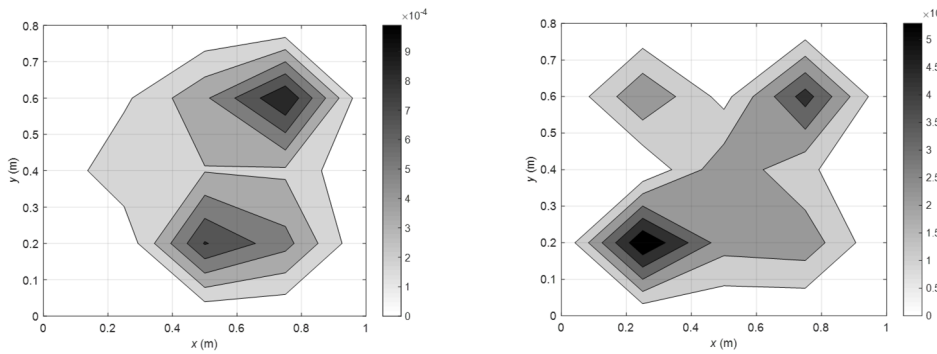

a) Before control b) After control

Fig. 7. The vibration velocity distributions on the plate (100 Hz)

ISSN PRINT 1392-8716, ISSN ONLINE 2538-8460

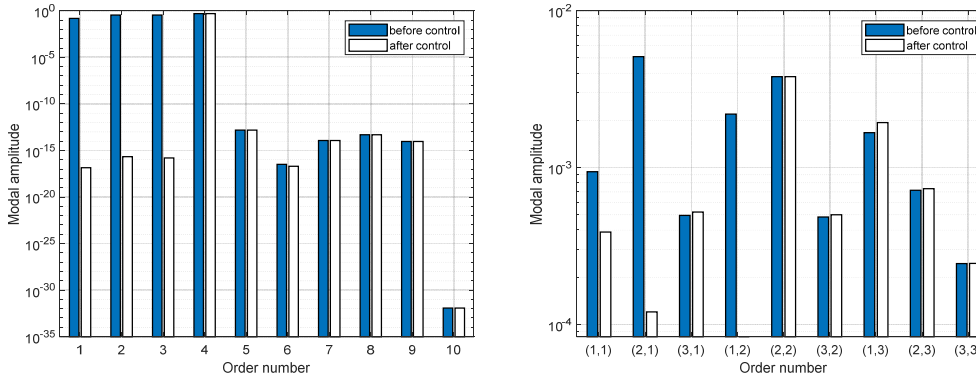

a) Amplitude of FRMs b) Amplitude of SMs

Fig. 8. Comparison of amplitudes of FRMs and SMs before and after the control (100 Hz)

4. Conclusions

By virtue of intuitively representation of relationship between excitation force and radiated sound power, FRM is introduced into ASAC in this paper, and an FRM based ASAC method is proposed by configuring the control force distribution to make the total excitation force vector orthogonal to each FRM. Detailed theoretical study and numerical simulation are conducted, and some conclusions can be drawn as follows.

1) The radiated sound power can be decoupled by the FRMs, and the control force distribution requirements can be conveniently obtained. Hence, the presented ASAC method based on FRM can greatly simplify the control system and improve the control effect and robustness.

2) At the modal frequencies, the sound radiation and vibration of the plate can both be controlled effectively at the same time when the 1st FRM is controlled.

3) At the non-modal frequencies, the sound radiation of the plate can be attenuated greatly by controlling the first several FRMs with relatively large eigenvalues, while the vibration control effect is not assured as good as that at the modal frequency.

Acknowledgements

The authors have not disclosed any funding.

Data availability

The datasets generated during and/or analyzed during the current study are available from the corresponding author on reasonable request.

Author contributions

Rongfu Mao: conceptualization. Haichao Zhu: supervision. Shanping Gao: methodology. Xing Zhang: validation.

Conflict of interest

The authors declare that they have no conflict of interest.

References

[1] C. R. Fuller, C. H. Hansen, and S. D. Snyder, "Active control of sound radiation from a vibrating rectangular panel by sound sources and vibration inputs: An experimental comparison," *Journal of*

Sound and Vibration, Vol. 145, No. 2, pp. 195–215, Mar. 1991, https://doi.org/10.1016/0022-460x(91)90587-a

[2] T. Y. Wu and Y. L. Chung, "Structural acoustic reduction via piezoelectric actuation and adaptive eigenvector optimization algorithm," *Journal of Intelligent Material Systems and Structures*, Vol. 21, No. 18, pp. 1797–1808, Nov. 2010, https://doi.org/10.1177/1045389x10389206

[3] J. Bai, S. Li, and M. L. Xia, "Active structural acoustic control based on the left eigenvector configuration," (in Chinese), *Journal of Vibration and Shock*, Vol. 37, No. 1, pp. 66–71, 2018, https://doi.org/10.13465/j.cnki.jvs.2018.01.011

[4] Y. Cao, S. D. Sommerfeldt, W. Johnson, J. D. Blotter, and P. Ashlani, "An analysis of control using the weighted sum of spatial gradients in active structural acoustic control for flat panels," *The Journal of the Acoustical Society of America*, Vol. 138, No. 5, pp. 2986–2997, Nov. 2015, https://doi.org/10.1121/1.4934730

[5] C. Hesse, V. Papantoni, S. Algermissen, and H. P. Monner, "Frequency-independent radiation modes of interior sound radiation: Experimental study and global active control," *Journal of Sound and Vibration*, Vol. 401, pp. 204–213, Aug. 2017, https://doi.org/10.1016/j.jsv.2017.04.038

[6] C. W. Su, H. C. Zhu, and R. F. Mao, "Determination method of dominant acoustic radiation modes in coupling enclosure," (in Chinese), *Journal of National University of Defense Technology*, Vol. 41, No. 2, pp. 158–162, Apr. 2019, https://doi.org/10.11887/j.cn.201902023

[7] O. Jeon, H.-G. Kim, J. Kook, S. M. Kim, and S. Wang, "Active structural acoustic control for radiated sound power reduction of enclosure with vent holes based on radiation modes," *Journal of Mechanical Science and Technology*, Vol. 36, No. 7, pp. 3313–3327, Jul. 2022, https://doi.org/10.1007/s12206-022-0611-y

[8] M. A. Nouh, O. J. Aldraihem, and A. Baz, "Periodic metamaterial plates with smart tunable local resonators," *Journal of Intelligent Material Systems and Structures*, Vol. 27, No. 13, pp. 1829–1845, Jul. 2016, https://doi.org/10.1177/1045389x15615965

[9] K.-C. Chuang, X.-F. Lv, and Y.-H. Wang, "A bandgap switchable elastic metamaterial using shape memory alloys," *Journal of Applied Physics*, Vol. 125, No. 5, Feb. 2019, https://doi.org/10.1063/1.5065557

[10] X.-N. Zhao, X.-D. Yang, W. Zhang, and H. Pu, "Active tuning of elastic wave propagation in a piezoelectric metamaterial beam," *AIP Advances*, Vol. 11, No. 6, Jun. 2021, https://doi.org/10.1063/5.0039050

[11] Z. Yamaguchi, J. Stuart Bolton, and K. Sakagami, "Reduction of sound radiation by using force radiation modes," *Applied Acoustics*, Vol. 72, No. 7, pp. 420–427, Jun. 2011, https://doi.org/10.1016/j.apacoust.2011.01.006

[12] Z. Yamaguchi, K. Sakagami, M. Morimoto, and J. S. Bolton, "Experimental identification of force radiation modes," *Noise Control Engineering Journal*, Vol. 61, No. 1, pp. 81–86, Jan. 2013, https://doi.org/10.3397/1/1.3761008

[13] G. Ji, W. K. Zhang, Q. D. Zhou, and L. Tan, "Force radiation mode analysis and acoustic reduction of cylindrical structure," (in Chinese), *Journal of Naval University of Engineering*, Vol. 26, No. 4, pp. 83–87, Aug. 2014, https://doi.org/10.7495/j.issn.1009-3486.2014.04.020

[14] L. Fu, G. Ji, Q. D. Zhou, and Y. C. Pan, "The influence of driving force location on acoustic power radiated from a cylindrical shell," (in Chinese), *Technical Acoustics*, Vol. 36, No. 2, pp. 104–109, Apr. 2017, https://doi.org/10.16300/j.cnki.1000-3630.2017.02.002

Rongfu Mao received Ph.D. degree in Institute of Noise and Vibration from Naval University of Engineering, Wuhan, China, in 2010. Now he works at Quanzhou University of Information Engineering. His current research interests include noise control and acoustic source identification.

Haichao Zhu received Ph.D. degree in Department of Power Engineering from Naval University of Engineering, Wuhan, China, in 1995. Now he works at Naval University of Engineering. His current research interests include noise control and vibration isolation.

Shanping Gao received B.S. degree in College of Mechanical Engineering and Automation from Huaqiao University, Quanzhou, China, in 2020. Now he works at Quanzhou University of Information Engineering. His current research interests include mechanical manufacturing and automation.

Xing Zhang received Ph.D. degree in College of Naval Architecture and Power from Naval University of Engineering, Wuhan, China, in 2011. Now he works at Quanzhou University of Information Engineering. His current research interests include noise control and acoustic intelligent monitoring.